JVI Journals.ASM.org

Mast Cell-Induced Lung Injury in Mice Infected with H5N1 Influenza Virus

Yanxin Hu,[a] Yi Jin,[a,c] Deping Han,[a] Guozhong Zhang,[a] Shanping Cao,[a] Jingjing Xie,[a] Jia Xue,[a] Yi Li,[a] Di Meng,[a] Xiaoxu Fan,[a] Lun-Quan Sun,[b] and Ming Wang[a]

1 Key Laboratory of Zoonosis of Ministry of Agriculture, College of Veterinary Medicine, China Agricultural University, Beijing, China[a]; Center for Molecular Medicine, Xiangya Hospital, Central South University, Changsha, China[b]; and College of Biological Sciences and Biotechnology, Beijing Forestry University, Beijing, China[c]

Although an important role for mast cells in several viral infections has been demonstrated, its role in the invasion of highly pathogenic H5N1 influenza virus is unknown. In the present study, we demonstrate that mast cells were activated significantly by H5N1 virus (A/chicken/Henan/1/2004) infection both *in vivo* and *in vitro*. Mast cells could possibly intensify the lung injury that results from H5N1 infection by releasing proinflammatory mediators, including histamine, tryptase, and gamma interferon (IFN-γ). Lung lesions and apoptosis induced by H5N1 infection were reduced dramatically by treatment with ketotifen, which is a mast cell degranulation inhibitor. A combination of ketotifen and the neuraminidase inhibitor oseltamivir protected 100% of the mice from death postinfection. In conclusion, our data suggest that mast cells play a crucial role in the early stages of H5N1 influenza virus infection and provide a new approach to combat highly pathogenic influenza virus infection.

The rapid spread and high pathogenicity of avian influenza virus H5N1 have caused severe problems in domestic poultry and humans worldwide (7, 18, 23). The mortality rate for highly pathogenic H5N1 influenza virus infection in humans is >50%, and the symptoms in infected animals or humans include fever, inappetence, encephalitis, pneumonia, and acute respiratory distress syndrome (43, 44). Diffuse alveolar damage and hemorrhage in the lungs caused by overreactive inflammatory responses in infected patients are the major causes of mortality (25, 33). It has been reported that the lungs of H5N1-infected mice are infiltrated by many inflammatory cells, which play an important role in the early stages of infection (44). H5N1 nucleoprotein and hemagglutinin were identified in the nuclei and cytoplasm of neutrophils, and viral RNA was detected in neutrophils, which indicated that neutrophils may serve as a vehicle for viral replication and transportation in avian influenza (45). Macrophages contribute to the unusual severity of human H5N1 disease by producing tumor necrosis factor alpha (TNF-α) and other cytokines (9). More recently, a study conducted by Du et al. has demonstrated that natural killer (NK) cell activation can be triggered by H5N1-pseudotyped particles (12). Overproduction of inflammatory cytokines, such as TNF-α, interleukin 6 (IL-6), and CC chemokine ligand 2 (CCL2), has also been demonstrated in H5N1-infected mice or humans, and the "cytokine storm" has been widely hypothesized to be the main cause of pathology and, ultimately, of death (9, 26, 41). However, it is discouraging that inhibition of the cytokine response (TNF-α, IL-6, CCL2, TNF-α receptor 1, TNF-α receptor 2, macrophage inflammatory protein-1α, and IL-1 receptor) does not protect infected animals from lethal H5N1 influenza virus infection (5, 35). Thus, the mechanisms of inflammatory injury induced by H5N1 infection are still debated. It is highly likely that some other inflammatory factors might have been overlooked, such as mast cells and their mediators. As one of the key players in inflammation and the immune response, the role of mast cells in H5N1 influenza virus infection remains to be defined.

Mast cells are widely distributed in all tissues throughout the body and play a crucial role in the immune response and inflammation by production of many inflammatory molecules, including potent proteases, cytokines, chemokines, and arachidonic acid metabolites (29). Mast cells are best known for their potent effector functions in allergic diseases (4). Recently, the involvement of mast cells in tumors and parasitic, bacterial, and viral infections has attracted widespread attention. In particular, mast cells have been implicated in the pathogenesis of some viral infections, such as HIV-1, dengue virus, cytomegalovirus, and bovine respiratory syncytial virus (17, 22, 24, 36, 40). Mast cells can intensify immunological injury through the production of mediators, including tryptase, TNF-α, IL-6, IL-1, and CCL3 (10, 30). Despite clear indications that mast cells contribute to the pathology of several viral infections, it has yet to be determined what roles mast cells play in the inflammatory responses induced by influenza virus infection.

In the present study, we investigated whether mast cells play a role in the initial process of influenza virus infection and what contributions mast cells make to the pathological consequences of influenza viruses. We show that mast cells actively participate in the first-line immunological responses to infection. Through release of tryptase, histamine, and gamma interferon (IFN-γ), mast cells could aggravate pathological injury of the infected tissues by directly inducing apoptosis or inflammatory cytokines and mediators.

MATERIALS AND METHODS

Mice and cells. Female BALB/c mice 8 to10 weeks old were purchased from Vital River Laboratories (Beijing, China), and the original breeding pairs were from Charles River Laboratories. The mice were housed in

Received 18 August 2011 Accepted 27 December 2011
Published ahead of print 11 January 2012
Address correspondence to Ming Wang, vetdean@cau.edu.cn, or Lun-Quan Sun, lq-sun@hotmail.com.

doi:10.1128/JVI.06053-11

TABLE 1 *In vivo* treatment protocols

Group	Treatment protocol
Oseltamivir	Oseltamivir 200 μg in 200 μl (10 mg/kg) at 4 h postinfection twice daily for 8 days intragastrically
Oseltamivir+ Ketotifen	Oseltamivir 200 μg in 100 μl (10 mg/kg) plus ketotifen 200 μg in 100 μl (10 mg/kg) at 4 h postinfection twice daily for 8 days intragastrically
Ketotifen	Ketotifen 200 μg in 200 μl (10 mg/kg) at 4 h postinfection twice daily for 8 days intragastrically
PBS	PBS as a control

independent ventilated cages and received pathogen-free food and water. The experimentation with animals was governed by the Regulations of Experimental Animals of Beijing Authority and approved by the Animal Ethics Committee of the China Agricultural University.

The mouse lymphoblast-like mastocytoma P815 cell line, LA795 mouse adenocarcinoma cell line, human lung adenocarcinoma epithelial A549 cell line, and Madin-Darby canine kidney (MDCK) cell line were provided by the Cell Resource Center of Peking Union Medical College. The cells were cultured and maintained according to the supplier's recommendations.

Chemicals. Ketotifen was purchased from Sigma (Shanghai, China) (K2628), dissolved in 0.85% saline, and prepared fresh on the day of use. Oseltamivir phosphate (Tamiflu; Roche, Basel, Switzerland) was dissolved in 0.85% saline and administered to the mice in a dose of 10 mg/kg body weight. Anti-mouse IFN-γ biotin was purchased from Ebioscience (Beijing, China).

Virus and challenge. The H5N1 influenza virus (A/chicken/Henan/1/2004, clade 2) used in this study was isolated from infected chicken flocks. This strain of virus has six consecutive basic amino acids at the hemagglutinin (HA) cleavage site, and the receptor binding sites are exactly the same as in A/Hong Kong/156/97 (H5N1). The virus was isolated from Henan Province, China. The virus was propagated in Madin-Darby canine kidney cells at 37°C for 48 h, and the viral supernatant was harvested, aliquoted, and stored at −80°C. The 50% lethal dose (LD_{50}) was determined in mice after serial dilution of the stock. Virus stocks were diluted in phosphate-buffered saline (PBS). The mice were anesthetized with Zoletil (Virbac, Carros, France) and infected with 5 LD_{50} in 50 μl intranasally. P815 cells were washed with PBS, resuspended at 1×10^6 cells/ml in a six-well plate, and treated with 1 PFU/cell of H5N1 virus.

***In vivo* challenge assay.** In the ketotifen treatment study, mice (six mice per group) were administrated ketotifen (5, 10, and 25 mg/kg) intragastrically at 4 h postinfection (p.i.) twice daily for 8 days and observed for survival for 14 days. In the ketotifen-plus-oseltamivir study, a mixture of ketotifen (10 mg/kg) and oseltamivir (10 mg/kg) in a 200-μl total volume was given intragastrically to mice (12 mice per group) twice daily for 8 days. Control mice were given PBS at the same time. The lung tissues of three mice per group were collected on day 3 and day 8 postinfection for real-time PCR and histopathologic analysis. The bronchoalveolar lavage fluid (BALF) from three mice per group was collected, and the level of lactate dehydrogenase (LDH) was detected with an Accute TBA-40FR (Toshiba, Tokyo, Japan). Data analysis was performed using the Smart Lis software (Dragon Tech, Shenzheng, China) supplied with the instrument. Six mice per group were observed for survival for 14 days. The details of the treatment schedule for each group are shown in Table 1.

Plaque assay. MDCK cells were cultured in Dulbecco's modified Eagle's medium (DMEM) (HyClone Laboratories, Utah) containing 10% fetal bovine serum (FBS) (HyClone Laboratories), 100 U/ml penicillin, and 100 μg/ml streptomycin. The BALF from individual mice was diluted 10-fold and added to a monolayer of MDCK cells in semisolid agar that contained 0.5 μg/ml trypsin tosylsulfonyl phenylalanyl chloromethyl ketone (TPCK) (Sigma, Beijing, China). Cultures were incubated at 37°C and 5% CO_2 for 60 to 72 h, fixed, and stained with 1% crystal violet. The plaques were counted.

Histology and immunochemistry. Lungs, nose, trachea, and hilar lymph nodes were removed from the euthanized mice and fixed in 4% neutral formalin at room temperature for 48 h. Serial tissue sections 5 μm thick were obtained after embedding in paraffin. Each slide was stained with hematoxylin and eosin (H&E), or toluidine blue for mast cells (42a). The mast cells in the sections were counted under a light microscope at ×10 magnification, and the mean was calculated. Tissue sections were stained as described previously (19b) using an anti-influenza virus nucleoprotein monoclonal antibody (MAb) (AA5H; Abcam, Hong Kong, China) or anti-mouse tryptase (Calbiochem Merck KGaA Co., Germany) or -TNF-α (Chemicon, Rosemont) MAb at 1:1,000, 1:400, or 1: 500 dilution, respectively. All sections were examined by light microscopy (CX31; Olympus, Tokyo, Japan). The expression of tryptase and TNF-α was semiquantitatively analyzed under a light microscope at ×40 magnification. The total visual areas (*A*) were traced randomly, and the total areas (*B*) of the positive cells in the visual area were determined using an image analyzer (SP500 high-speed color image analyzer; Olympus, Tokyo, Japan). The results were expressed as a percentage of *B* divided by *A*.

P815 cell degranulation detection. P815 cell degranulation was quantified by measuring tryptase activity in culture supernatants and lysates of cells stimulated or not with H5N1 virus for 24 h, using a Mast Cell Degranulation Assay Kit (Chemicon International).

Viral RNA determination by real-time PCR. Total RNA was prepared from 10 mg lung tissue homogenized in TRIzol reagent (Invitrogen, Utah) according to the manufacturer's instructions. DNase I-treated RNA (0.2 μg) was reverse transcribed into cDNA using random primer or universal primers for influenza A virus (Uni12) (19a). Real-time PCR was performed to amplify the HA gene of H5N1 influenza virus using the Power SYBR Green PCR Master Mix kit (ABI, California). The following primers were used in the PCRs: forward primer, 5′-CGCAGTATTCAGAAGAAGCAAGAC-3′; reverse primer, 5′-TCCATAAGGATAGACCAGCTACCA-3′. The reaction was run on an ABI 7500 with the following steps: 95°C for 10 min and 40 cycles of denaturation at 95°C for 15 s, annealing at 56°C for 30 s, and extension at 72°C for 40 s. Data analysis was performed using the 7500 software (version 2.0; ABI, California) supplied with the instrument. The copy number of the HA gene was calculated using an HA-containing plasmid of known concentration as a standard.

The real-time PCR primers for β-actin and IFN-γ were 5′-GAGACCTTCAACACCCCGC-3′ and 5′-ATGTCACGCACGATTTCCC-3′ (β-actin) and 5′-AGTGGCATAGATGTGGAA-3′ and 5′-GACCTGTGGGTTGTTGA-3′ (IFN-γ). Reactions were carried out with initial denaturation at 95°C for 10 min and then 40 cycles of denaturation at 95°C for 15 s, annealing at 50°C for 30 s, and extension at 72°C for 40 s. Gene expression was normalized to that of the control group using the $2^{-\Delta\Delta CT}$ method with β-actin as an internal standard.

Histamine detection. The content of histamine in tissues can be determined by the fluorescence intensity. A fluorometric method was used for the determination of histamine as described previously (42a).

TUNEL staining. Apoptotic cells were examined by using the In Situ Cell Death Detection kit (Roche, Philadelphia, PA). Paraffin slides of lung tissues were dewaxed, rehydrated according to standard procedures, and immersed in a plastic jar containing 200 ml citrate buffer (0.1 M, pH 6.0). The slides were subjected to 750 W (high) microwave irradiation for 1 min, cooled rapidly by immediately adding 80 ml double-distilled water (20 to 25°C), and then transferred into PBS (20 to 25°C). The slides were immersed for 30 min at 15 to 25°C in Tris-HCl (0.1 M, pH 7.5, which contained 3% bovine serum albumin [BSA] and 20% normal bovine se-

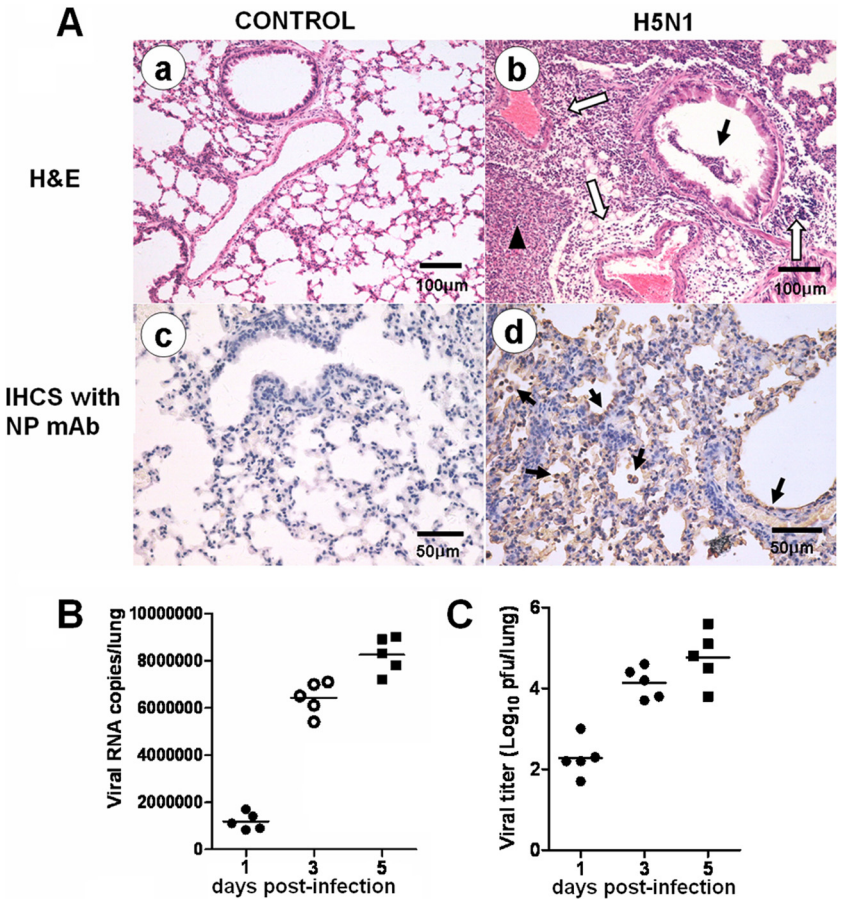

FIG 1 Pathological features of H5N1-infected mice. (A) Lung histopathology at 5 days p.i. Representative lung sections from each group were subjected to H&E staining or immunohistochemical (IHCS) staining with an anti-influenza virus NP MAb. (a) Normal lung without pathological changes. (b) The open arrows indicate interstitial edema and inflammatory cell infiltration around small blood vessels; the solid arrow indicates dropout of mucous epithelium in the bronchioles; the arrowhead indicates edema and infiltration of epithelial cells, erythrocytes, and inflammatory cells in the alveolar lumen. (c) Normal lung without NP-positive cells. (d) The arrows indicate NP-positive cells. (B and C) Three mice were euthanized on days 1, 3, and 5 p.i., and the viral titers in the lungs were determined by real-time PCR (B) and plaque assay (C). The horizontal lines indicate the average value of three measurements.

rum) and then rinsed twice with PBS at 15 to 25°C. The terminal deoxynucleotidyltransferase-mediated dUTP-biotin nick end labeling (TUNEL) reaction mixture was added to the slides and incubated at 37°C in a humidified atmosphere in the dark for 60 min. The slides were rinsed three times in PBS for 5 min each time. Samples were analyzed in a drop of PBS under a fluorescence microscope, with excitation at 450 to 500 nm and detection at 515 to 565 nm (green). For the negative control, the TUNEL reaction mixture was replaced with label solution. The numbers of positive cells were quantitatively analyzed under a light microscope at ×10 magnification.

Cytokine measurement with a BD CBA Flex Set. Supernatants were obtained at 24 and 48 h after P815 cells were infected with H5N1 virus. The supernatants were tested for IL-6, TNF-α, IFN-γ, IL-1β, and IL-12 according to the manufacturer's protocol. Data acquisition and analysis were performed on a fluorescence-activated cell sorter (FACS) LSRII using FACSDiva software (BD Biosciences, California).

Analysis of LA795 and A549 cell apoptosis by flow cytometry. P815 cells were infected with H5N1 virus (1 PFU/cell), and 48 h later, the supernatant was collected. LA795 and A549 cells were incubated with the supernatant, and apoptosis was detected at the 24-h and 48-h time points by flow cytometry using a fluorescein isothiocyanate (FITC) Annexin V Apoptosis Detection Kit II (BD Biosciences, California).

Statistical analysis. Statistical analysis was performed by one-way analysis of variance (ANOVA) contained in the SPSS software suite (version 12.0; SPSS Taiwan Corp., Taiwan), and a P value of <0.05 was considered statistically significant. Results are expressed as means and standard deviations.

RESULTS

Mast cells involved in H5N1 influenza virus infection. We used a mouse H5N1 virus (A/chicken/Henan/1/2004) infection model to study the roles of mast cells (Fig. 1). These mice presented typical clinical signs of inactivity, ruffled hair, inappetence, emaciation, and labored respiration on day 5 p.i. Gross observation of H5N1-infected mice demonstrated that the lungs were highly edematous, with pervasive hemorrhage. The lung lesions of H5N1-infected mice were characterized by interstitial edema and inflammatory cell infiltration around small blood vessels, exfoliation of bronchiolar epithelium, thickened alveolar walls, and flooded edema fluid mixed with epithelial cells, erythrocytes, and inflammatory cells in the alveolar lumen (Fig. 1A, b). The H5N1 viral antigen (42) was detected extensively in the deciduous alveolar cells and mucosal epithelial cells in the lung (Fig. 1A, d). H5N1 viral replication increased over time postinfection, as determined by real-time reverse transcription (RT)-PCR (Fig. 1B) and plaque assay (Fig. 1C).

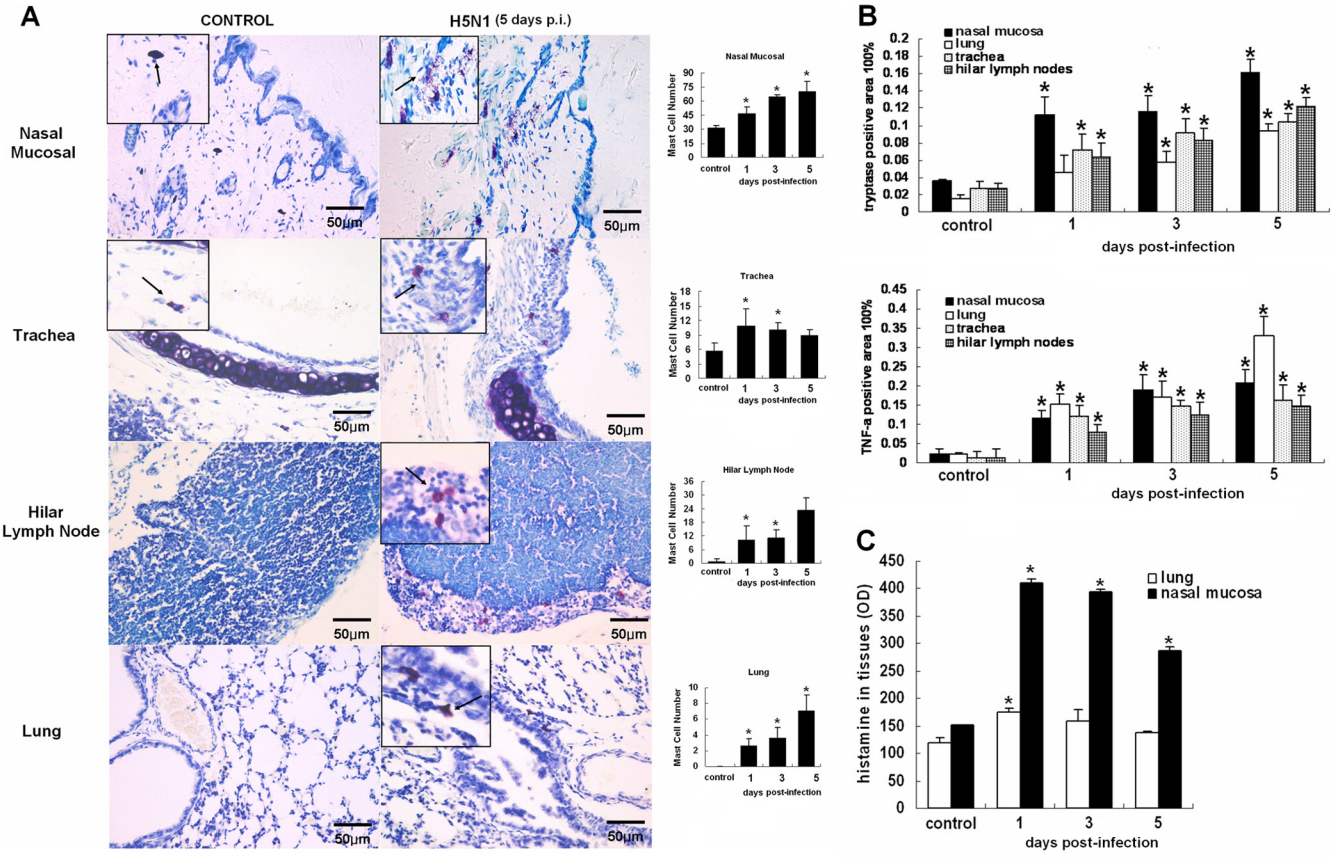

FIG 2 Distribution of mast cells and tryptase, TNF-α, and histamine levels in tissues of H5N1-infected mice. (A) Distribution of mast cells after infection. Representative sections of the nasal mucosa, trachea, hilar lymph node, and lung from each group were stained with toluidine blue for mast cells; the arrows indicate the mast cells. The numbers of mast cells from whole tissue sections are graphed on the right ($n = 5$). The error bars indicate standard deviations. (B) Expression of tryptase and TNF-α on days 1, 3, and 5 p.i. in different tissues of the nasal mucosa, trachea, hilar lymph node, and lung ($n = 5$). (C) Levels of histamine in different tissues of the nasal mucosa and lung on days 1, 3, and 5 postinfection. *, $P < 0.05$ compared with the control group.

In the infection model, the numbers of mast cells in the nasal mucosa, trachea, hilar lymph nodes, and lung increased dramatically ($P < 0.05$) on days 1, 3, and 5 p.i. (Fig. 2A). Typical degranulation was observed in the infected nasal mucosa and trachea in infected mice. We examined the levels of the mediators released by activated mast cells. As shown in Fig. 2B, levels of tryptase and TNF-α in the nasal mucosa, trachea, hilar lymph nodes, and lungs of infected mice increased significantly on days 1, 3, and 5 p.i. ($P < 0.05$) compared with the control group. The histamine level in the nasal mucosa was significantly increased in infected mice on days 1, 3, and 5 p.i. ($P < 0.05$), which was consistent with the number of mast cells in the nasal mucosa. However, the histamine level in the lungs of the infected mice peaked on day 1 p.i. ($P < 0.05$), declined on day 2 p.i., and approached the basal level on day 5 p.i. (Fig. 2C).

Inhibition of mast cell degranulation reduced lung lesions and apoptosis in pulmonary epithelial cells. To investigate whether mast cells were activated by H5N1 virus (A/chicken/Henan/1/2004) infection, we used the mast cell inhibitor ketotifen. Mice were given ketotifen (1 mg/kg body weight) once daily for 3 days by oral gavage, and all mice were challenged with 5 LD_{50} of H5N1 virus at 4 h after the first dose of ketotifen. Remarkably, we found that ketotifen treatment significantly reduced the lung lesions (Fig. 3A). Mice without ketotifen treatment showed severe bronchiolitis, peribronchiolitis, and bronchopneumonia, which were characterized by dropout and necrosis of mucous epithelial cells in the bronchioles; infiltration of various inflammatory cells, including lymphocytes, neutrophils, and plasmacytes near the small blood vessels; interstitial edema; thickening of the alveolar walls; and alveolar lumen flooding with dropout of alveolar cells, erythrocytes, and inflammatory cells in the lung. In comparison, the lungs of the mice with ketotifen treatment demonstrated only mild pathological lesions, such as mild bronchiolitis, which was characterized by dropout and necrosis of mucous epithelial cells in the bronchioles and inflammatory cell infiltration around the bronchioles and small blood vessels.

Pulmonary epithelial cell apoptosis was one of the key mechanisms by which influenza virus caused the lung lesions (6). We hypothesized that mitigation of the lung lesions by ketotifen was probably due to its impact on pulmonary epithelial cell apoptosis. To test this hypothesis, apoptotic cells in the lungs were examined by TUNEL staining. As shown in Fig. 3B, lung sections from H5N1-infected mice showed extensive apoptotic cells from day 3 to day 5 p.i. (Fig. 3B, b and c). In contrast, the number of apoptotic cells decreased in the lungs of ketotifen-treated mice from day 3 to day 5 p.i. (Fig. 3B, e and f), with the decrease in apoptotic cells

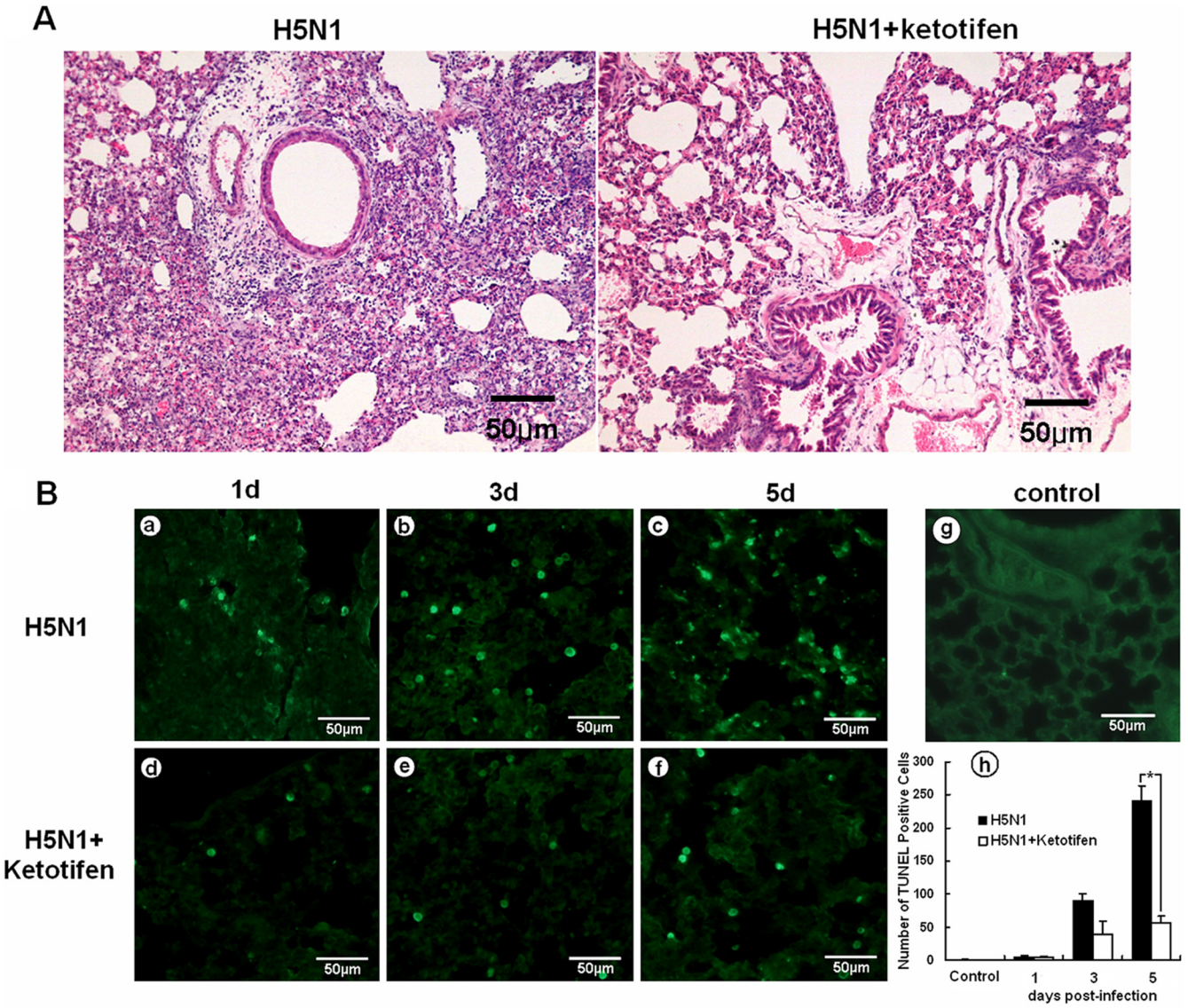

FIG 3 Lung histopathology and apoptosis from mice with or without ketotifen treatment. (A) Lung histopathology from mice without ketotifen treatment (left) and with treatment (right) at 5 days p.i. Sections stained with H&E and reduced lung lesions could be seen for the mice with ketotifen treatment. (B) Apoptosis of lung cells on days (d) 1, 3, and 5 p.i., as shown by TUNEL staining. Decreased apoptosis was seen, and a summary of the number of apoptotic cells is shown (h) ($n = 5$). The error bars indicate standard deviations. *, $P < 0.05$ compared with the control group (g).

being significant at day 5 ($P < 0.05$) (Fig. 3B, h). The results suggested that ketotifen reduced the lung lesions of H5N1-infected mice by inhibiting mast cell degranulation, which led to weakened apoptosis of pulmonary epithelial cells.

Having demonstrated that activated mast cells promoted lung lesions in mice during H5N1 infection by stimulating pulmonary epithelial cell apoptosis, we proceeded with a series of *in vitro* experiments to investigate further the cellular and biochemical changes in activated mast cells induced by H5N1 virus. First, we assayed degranulation by measuring tryptase activity in culture supernatants and lysates from the P815 mast cell line infected by H5N1 virus. Tryptase activity in the supernatants and lysates increased significantly at 24 h p.i. ($P < 0.05$) (Fig. 4A), which showed direct evidence of the activation of mast cells by H5N1 virus infection *in vitro*, consistent with the results *in vivo*.

To investigate whether the mediators released by activated P815 cells could induce pulmonary epithelial cell apoptosis, we used the supernatant of the infected P815 cells to culture LA795 (a mouse lung cell line) and A549 (a human lung cell line) cells and analyzed the apoptosis rates using FACS. The supernatants were collected at 48 h p.i. from P815 cells and prepared by ultracentrifugation for 3 h at 30,000 rpm to remove viral particles. By RT-PCR and plaque assay, no viral RNA or infectious viral particles were detected in the supernatants. When LA795 or A549 cells were treated with the supernatants, apoptosis rates increased significantly at 24 and 48 h ($P < 0.05$) (Fig. 4B). These data confirmed that the mediators released by activated mast cells induced apoptosis of LA795 and A549 cells.

To explore further which mediators were released by activated mast cells, cell-free supernatants from H5N1-infected P815 cells were analyzed by FACS for levels of apoptosis-related cytokines,

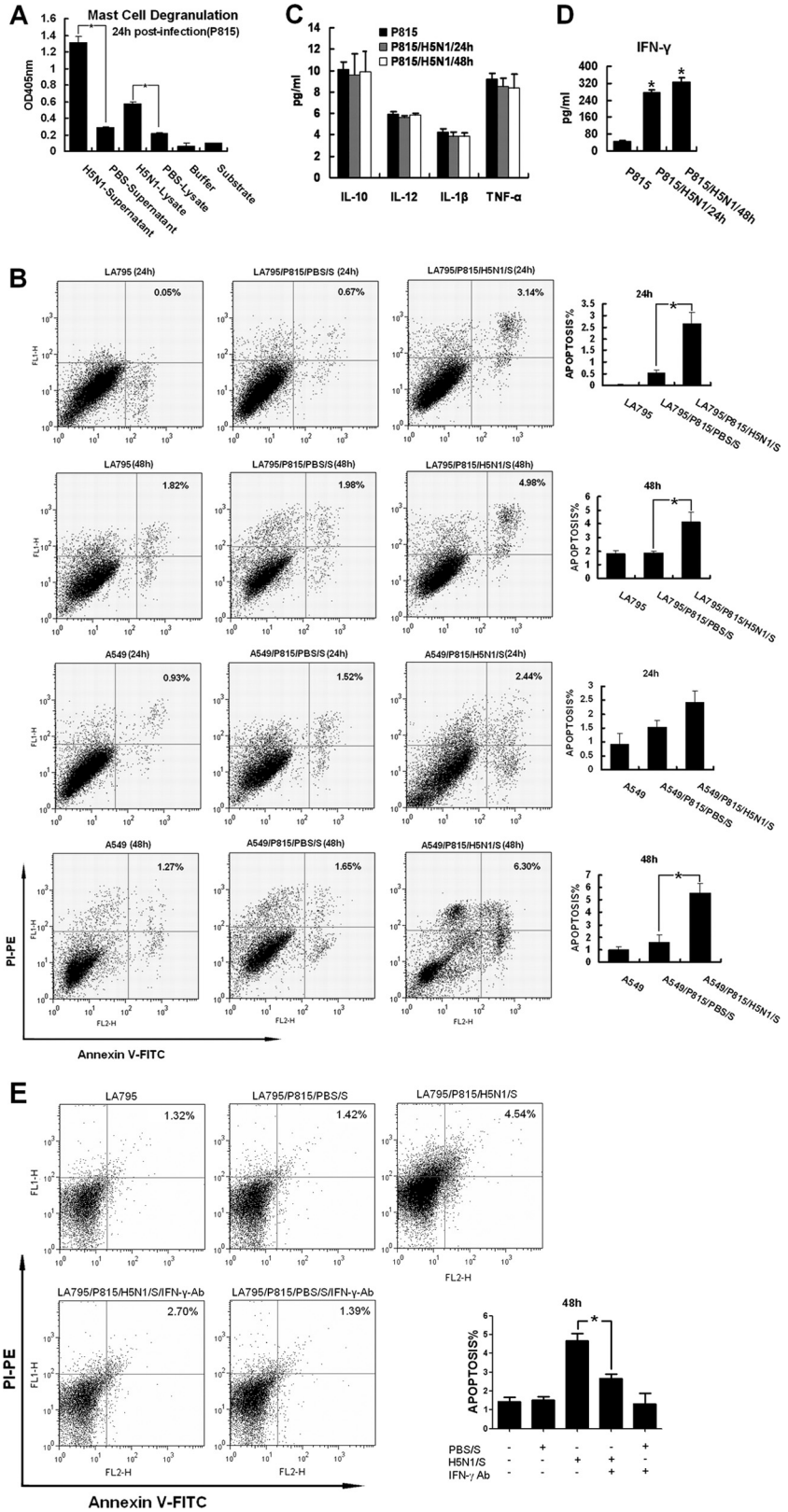

FIG 4 H5N1 virus activated mast cels *in vitro*. (A) P815 cell degranulation detected with a Mast Cell Degranulation Assay Kit at 24 h p.i. (B) Apoptosis of LA795 and A549 cells was analyzed by FACS using a FITC Annexin V Apoptosis Detection Kit II after stimulation with H5N1-infected P815 cell supernatant. (C) H5N1 infection induced IL-6, TNF-α, IL-1β, and IL-12 production by P815 cells that was detected by FACS. (D) H5N1 infection induced IFN-γ production by P815 cells that was detected by FACS. (E) Apoptosis rates of LA795 cells cultured by IFN-γ-blocked supernatants were analyzed by FACS using a FITC Annexin V Apoptosis Detection Kit II. The error bars indicate standard deviations.*, $P < 0.05$; $n = 3$.

including IL-6, TNF-α, IFN-γ, IL-1β, and IL-12. IFN-γ increased dramatically at 24 and 48 h p.i. ($P < 0.05$) (Fig. 4D); however, the levels of IL-6, TNF-α, IL-1β, and IL-12 did not change (Fig. 4C). These data indicated that IFN-γ is a key cytokine that plays an important role in pulmonary epithelial cell apoptosis and the lung lesions caused by activated mast cells.

To confirm the function of IFN-γ, an antibody blockage assay was performed. Cell-free supernatants from H5N1-infected P815 cells were treated with 10 μg/ml IFN-γ antibody. The apoptosis rates of LA795 cells cultured by IFN-γ-blocked supernatants were analyzed at 48 h. When LA795 cells were treated with the IFN-γ-blocked supernatants (Fig. 4E, LA795/P815/H5N1/S/IFN-γ-Ab), apoptosis rates were significantly lower than in the activated-supernatant-treated cells (LA795/P815/H5N1/S). These results further illustrated the important role of IFN-γ released by activated mast cells.

Inhibition of mast cell function improved the antiviral efficacy of oseltamivir in mice. Having demonstrated that ketotifen reduced the lung lesions and apoptosis in H5N1-infected mice, we further investigated whether it protected mice from H5N1 virus (A/chicken/Henan/1/2004) infection. Mice were given ketotifen (5, 10, and 25 mg/kg) twice daily for 8 days by oral gavage, starting at 4 h before viral challenge with 5 LD_{50} of the virus. Survival in each group was monitored for 14 days. As shown in Fig. 5A, 10 mg/kg was the most efficient dose against H5N1 virus (83.33% survival rate), whereas 5 mg/kg and 25 mg/kg provided 67.7% and 60.0% survival, respectively.

Based on the dose-response data, we selected 10 mg/kg ketotifen for combination therapy for H5N1 infection in mice. Animals were treated with ketotifen (10 mg/kg) and oseltamivir (10 mg/kg, a suboptimal dose determined in a pilot study). Combined administration of ketotifen and oseltamivir completely protected 100% of the mice from H5N1-induced death (Fig. 5B). The bodyweights of the mice treated with ketotifen plus oseltamivir were higher than those of other groups (Fig. 5C).

The lung tissues and bronchoalveolar lavage fluid of mice in each group on day 3 and day 8 postinfection were collected. The levels of viral RNA, IFN-γ, and LDH and the viral titer in the mice receiving either combination therapy or monotherapy were measured on day 3 and day 8 postinfection. Compared with the animals receiving monotherapy with either ketotifen or oseltamivir phosphate, viral replication (Fig. 5D and E) and the LDH level (Fig. 5G) were markedly suppressed in mice receiving combination therapy on day 8 postinfection ($P < 0.05$). Relative to the PBS group, the level of IFN-γ was significantly lower than that in the groups receiving monotherapy with ketotifen (Fig. 5F) on both day 3 and day 8 postinfection ($P < 0.05$). These results were consistent with the animal survival data. Fig. 5H shows the histopathological changes in the lungs of the mice in each group at day 8 postinfection. The serious lung lesions of the PBS group were characterized by dropout and necrosis of mucous epithelial cells in the bronchioles, infiltration of a large number of inflammatory cells near the small blood vessels and bronchioles, interstitial edema, thickening of the alveolar walls, and alveolar lumen flooding with dropout of alveolar cells, erythrocytes, and inflammatory cells in the lung (Fig. 5H, a). In mice that were treated with ketotifen or oseltamivir alone, fewer lung lesions were observed, but there was still some dropout and necrosis of mucous epithelial cells in the bronchioles and infiltration of inflammatory cells around the small blood vessels and bronchioles (Fig. 5H, b and c). In comparison, the lungs from mice with combination therapy showed only mild pathological lesions, such as peribronchovascular congestion (Fig. 5H, d). These results suggested that the combination treatment with ketotifen plus oseltamivir could significantly reduce the inflammation and lung lesions in the H5N1-infected mice.

DISCUSSION

Mast cells have been implicated in the pathogenesis of some viral infections. For example, mast cells may provide a viral reservoir that can be reactivated by stimuli, such as Toll-like-receptor-mediated signaling in HIV infection (40). Previous studies have demonstrated that H5N1 influenza virus infection causes a severe inflammatory response in the lung, accompanied by infiltration of various inflammatory cells, including lymphocytes, neutrophils, eosinophils, macrophages, NK cells, and plasmacytes (12, 44, 45). As far as we are aware, the present study is the first to demonstrate the direct involvement of mast cells in H5N1 infection, showing increased mast cell numbers in the nasal mucosa, trachea, and lungs during the early stage of infection with H5N1 influenza virus in mice. This suggests that mast cells serve as a primary detector of tissue infection or invasion and release proinflammatory mediators that recruit leukocytes to the appropriate site at risk (15). Mast cells have been shown to express TLR3, melanoma differentiation-associated gene 5, and retinoic acid-inducible gene 1 (RIG 1) and can be activated by Newcastle disease virus and dengue virus (32, 38). As for how mast cells are activated in the context of H5N1 infection, we speculate that the interactions between the virus RNA sensors on mast cells, such as TLR3, RIG 1, and H5N1 viral RNA, may contribute to the activation process, which has yet to be determined.

Activated mast cells release large amounts of mediators, including tryptase, histamine, and cytokines, such as IL-1β, IL-2, IL-3, IL-6, TNF-α, and IFN-γ (10, 29). Tryptase is the most abundant component of mast cell granules and is released when mast cells undergo degranulation. It has been reported that the level of tryptase has a profound biological affect on the inflammatory response (16). Moreover, previous studies have shown that tryptase from activated mast cells can stimulate secretion from neighboring mast cells and thus induce a feedback cycle as the disease progresses (19). Our data revealed that a large quantity of tryptase accumulated in the nasal mucosa, trachea, hilar lymph nodes, and lungs in H5N1-infected mice, which suggests that the release of tryptase is associated with a severe inflammatory response to H5N1 infection.

Histamine is a multifunctional biogenic amine that is mainly produced by mucosal mast cells and can contribute to the progression of inflammatory responses by enhancement of the secretion of proinflammatory cytokines, such as IL-1α, IL-1β, and IL-6, in several cell types and in local tissues (2). Moreover, mast cells are involved in repair of mucosal injury mediated by histamine release (3). The results from the current study showed that the histamine contents in the nasal mucosa and lungs of the infected mice increased during the course of infection, thus providing further evidence to link mast cells to the highly pathogenic features of H5N1 infection.

TNF-α has been shown to be elevated during influenza virus infection. In this study, the expression of TNF-α in H5N1-infected tissue was detected on days 1, 3, and 5 p.i., which was consistent with previous studies (42, 44). Unexpectedly, the sub-

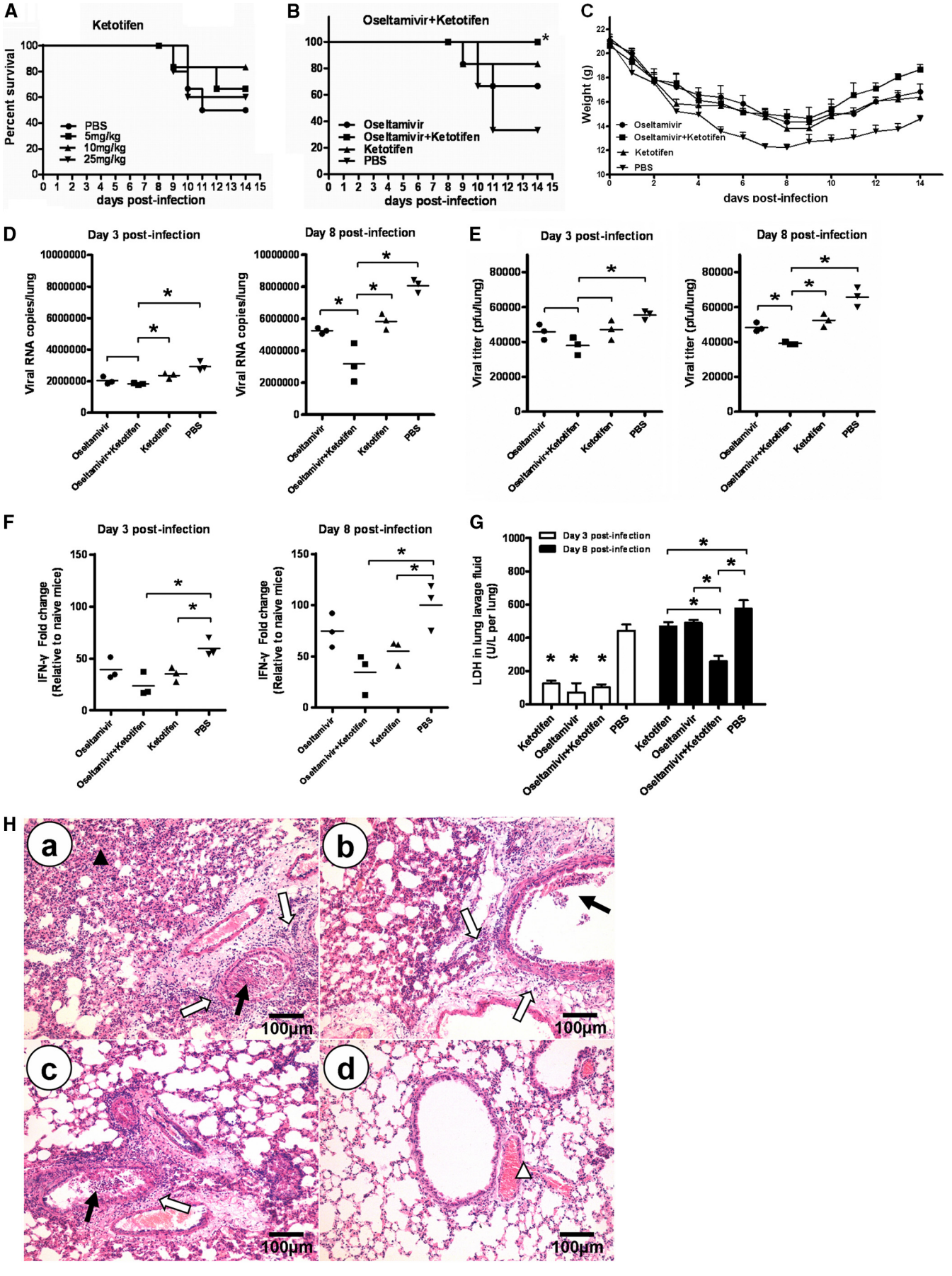
A
Ketotifen
Percent survival
PBS
5mg/kg
10mg/kg
25mg/kg
days post-infection
B
Oseltamivir+Ketotifen
Oseltamivir
Oseltamivir+Ketotifen
Ketotifen
PBS
days post-infection
C
Weight (g)
Oseltamivir
Oseltamivir+Ketotifen
Ketotifen
PBS
days post-infection
D
Day 3 post-infection
Day 8 post-infection
Viral RNA copies/lung
Oseltamivir
Oseltamivir+Ketotifen
Ketotifen
PBS
E
Day 3 post-infection
Day 8 post-infection
Viral titer (pfu/lung)
F
Day 3 post-infection
Day 8 post-infection
IFN-γ Fold change (Relative to naive mice)
G
Day 3 post-infection
Day 8 post-infection
LDH in lung lavage fluid (U/L per lung)
H
a
b
c
d
100μm

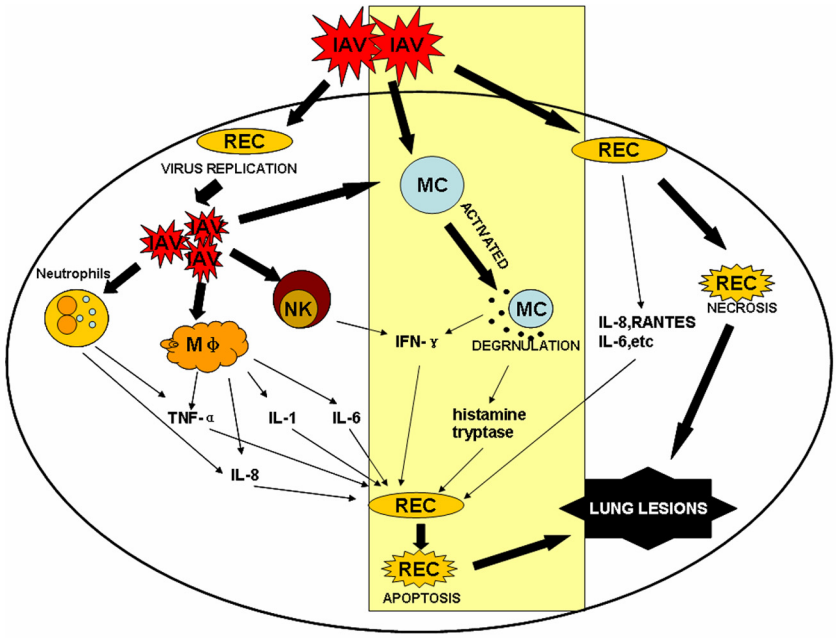

FIG 6 Major inflammatory cells and cytokine infiltration in influenza A virus infection. The rectangle with the pale yellow shading indicates the findings in the present study about the role of mast cells in influenza virus infection. IAV, influenza A virus; REC, respiratory epithelial cell; MC, mast cell; Mφ, macrophage.

sequent *in vitro* experiment revealed that the increased level of TNF-α was not from the H5N1-activated mast cells, although there is evidence that TNF-α can be released by activated mast cells in many other infections (13, 14). However, our data further showed that abundant IFN-γ was released by H5N1-infected mast cells *in vitro*. It has been well documented that influenza virus induces high levels of IFN-γ in the lungs of infected animals, which is believed to be produced mainly by T and NK cells (1, 42). In the present study, we demonstrated that mast cells released a high level of IFN-γ after H5N1 virus infection *in vitro*, and this is believed to be the first report that IFN-γ can be produced by activated mast cells, in addition to T and NK cells, in H5N1 virus infection. Furthermore, many data have shown that IFN-γ can induce apoptosis of pulmonary epithelial cells, immune cells, and tumor cells (12, 27, 37, 39, 46). Our results suggested that activated mast cells probably promoted apoptosis of the pulmonary epithelial cells by releasing IFN-γ. Based on our data and those of others, we propose that mast cells can be activated by H5N1 virus and that mast cells proliferate and release many mediators, including histamine, tryptase, and IFN-γ. The mediators can induce inflammatory responses and aggravate pathological injury of the infected tissues directly or via induction of apoptosis, together with lymphocytes, neutrophils, eosinophils, macrophages, and NK cells (Fig. 6).

Several antiviral agents, such as zanamivir (Relanza) and oseltamivir (Tamiflu), have been shown to be effective against influenza virus clinically, but the gradual emergence of drug-resistant strains could restrict their therapeutic benefits (8, 11, 28). Combination therapy with the drugs might provide some advantages over monotherapy, because different drugs interfere with different stages of the virus replication cycle or affect different aspects of virus pathogenicity. Ilyushina et al. have reported that combination treatment with 10 mg/kg/day oseltamivir and 37.5 mg/kg/day ribavirin completely inhibited virus replication in mice infected with H5N1 influenza virus (20). Combination treatment with amantadine (15 or 30 mg/kg/day) and oseltamivir (10 mg/kg/day) provided greater protection (60% and 90%, respectively) against lethal infection with amantadine-sensitive H5N1 virus than did monotherapy (21). Here, we found that inhibition of mast cell degranulation effectively protected mice from death after H5N1 infection, probably by reducing the lung lesions and by inhibition of apoptosis, which was evidenced by a decreased level of IFN-γ in ketotifen-treated groups. The results suggest that the mast cell degranulation inhibitor is a potent antiviral agent against influenza virus. We found that a combination of ketotifen (10 mg/kg) and oseltamivir (10 mg/kg) protected 100% of the mice from death caused by H5N1 infection, which offers an alternative strategy for controlling a potential pandemic influenza outbreak.

FIG 5 Therapeutic effect of ketotifen on H5N1 infection in mice. (A) Survival rates of H5N1-infected mice after treatment with different doses of ketotifen ($n = 6$). (B) Survival rates of H5N1-infected mice after treatment with combined ketotifen and oseltamivir ($n = 6$; *, $P < 0.05$ by log rank analysis). (C) Bodyweights were recorded daily. The error bars indicate standard deviations. (D, E, and F) Three mice in each group were euthanized on day 3 and day 8 postinfection, the viral titers in lungs were determined by real-time PCR (D) and plaque assay (E), and IFN-γ in lungs was determined by real-time PCR (F) ($n = 3$; *, $P < 0.05$). (G) The level of LDH in lung lavage fluid was determined with an Accute TBA-40FR ($n = 3$; *, $P < 0.05$). The horizontal lines indicate the average value of three measurements. (H) Lung histopathology on day 8 postinfection. Representative lung sections from each group were stained with H&E. The open arrows indicate interstitial edema and inflammatory cell infiltration, the solid arrows indicate dropout of mucous epithelium in the bronchioles, the open arrowhead indicates hemorrhage or congestion, and the solid arrowhead indicates thickening of the alveolar walls. a, PBS; b, ketotifen; c, oseltamivir; d, ketotifen plus oseltamivir.

ACKNOWLEDGMENTS

This work was supported by the Program for Cheung Kong Scholars and Innovative Research Teams in Chinese Universities (no. IRT0866) and the Chinese Universities Scientific Fund (2011JS010).

REFERENCES

1. **Aoyagi M, Shimojo N, Sekine K, Nishimuta T, Kohno Y.** 2003. Respiratory syncytial virus infection suppresses IFN-gamma production of gammadelta T cells. Clin. Exp. Immunol. **131**:312–317.
2. **Bayram H, et al.** 1999. Effect of loratadine on nitrogen dioxide-induced changes in electrical resistance and release of inflammatory mediators from cultured human bronchial epithelial cells. J. Allergy Clin. Immunol. **104**:93–99.
3. **Bechi P, et al.** 1995. Gastric mucosal histamine storing cells. Evidence for different roles of mast cells and enterochromaffin-like cells in humans. Dig. Dis. Sci. **40**:2207–2213.
4. **Bradding P, Walls AF, Holgate ST.** 2006. The role of the mast cell in the pathophysiology of asthma. J. Allergy Clin. Immunol. **117**:1277–1284.
5. **Carter MJ.** 2007. A rationale for using steroids in the treatment of severe cases of H5N1 avian influenza. J. Med. Microbiol. **56**:875–883.
6. **Chan MC, et al.** 2005. Proinflammatory cytokine responses induced by influenza A (H5N1) viruses in primary human alveolar and bronchial epithelial cells. Respir. Res. **6**:135.
7. **Chen H, et al.** 2006. Establishment of multiple sublineages of H5N1 influenza virus in Asia: implications for pandemic control. Proc. Natl. Acad. Sci. U. S. A. **103**:2845–2850.
8. **Cheung CL, et al.** 2006. Distribution of amantadine-resistant H5N1 avian influenza variants in Asia. J. Infect. Dis. **193**:1626–1629.
9. **Cheung CY, et al.** 2002. Induction of proinflammatory cytokines in human macrophages by influenza A (H5N1) viruses: a mechanism for the unusual severity of human disease? Lancet **360**:1831–1837.
10. **Dawicki W, Marshall JS.** 2007. New and emerging roles for mast cells in host defence. Curr. Opin. Immunol. **19**:31–38.
11. **de Jong MD, et al.** 2005. Oseltamivir resistance during treatment of influenza A (H5N1) infection. N. Engl. J. Med. **353**:2667–2672.
12. **Du N, et al.** 2010. Differential activation of NK cells by influenza A pseudotype H5N1 and 1918 and 2009 pandemic H1N1 viruses. J. Virol. **84**:7822–7831.
13. **Echtenacher B, Mannel DN, Hultner L.** 1996. Critical protective role of mast cells in a model of acute septic peritonitis. Nature **381**:75–77.
14. **Furuta T, Kikuchi T, Iwakura Y, Watanabe N.** 2006. Protective roles of mast cells and mast cell-derived TNF in murine malaria. J. Immunol. **177**:3294–3302.
15. **Gaboury JP, Johnston B, Niu XF, Kubes P.** 1995. Mechanisms underlying acute mast cell-induced leukocyte rolling and adhesion in vivo. J. Immunol. **154**:804–813.
16. **Galli SJ, Nakae S, Tsai M.** 2005. Mast cells in the development of adaptive immune responses. Nat. Immunol. **6**:135–142.
17. **Gibbons AE, Price P, Robertson TA, Papadimitriou JM, Shellam GR.** 1990. Replication of murine cytomegalovirus in mast cells. Arch. Virol. **115**:299–307.
18. **Guan Y, et al.** 2004. H5N1 influenza: a protean pandemic threat. Proc. Natl. Acad. Sci. U. S. A. **101**:8156–8161.
19. **He S, Gaca MD, Walls AF.** 1998. A role for tryptase in the activation of human mast cells: modulation of histamine release by tryptase and inhibitors of tryptase. J. Pharmacol. Exp. Ther. **286**:289–297.

19a. **Hoffmann E, Stech J, Guan Y, Webster RG, Perez DR.** 2001. Universal primer set for the full-length amplification of all influenza A viruses. Arch. Virol. **146**:2275–2289.

19b. **Hu Y, et al.** 2007. Effects of chronic heat stress on immune responses of the foot-and-mouth disease DNA vaccination. DNA Cell Biol. **26**:619–626.

20. **Ilyushina NA, et al.** 2008. Oseltamivir-ribavirin combination therapy for highly pathogenic H5N1 influenza virus infection in mice. Antimicrob. Agents Chemother. **52**:3889–3897.
21. **Ilyushina NA, Hoffmann E, Salomon R, Webster RG, Govorkova EA.** 2007. Amantadine-oseltamivir combination therapy for H5N1 influenza virus infection in mice. Antivir. Ther. **12**:363–370.
22. **Jolly S, Detilleux J, Desmecht D.** 2004. Extensive mast cell degranulation in bovine respiratory syncytial virus-associated paroxystic respiratory distress syndrome. Vet. Immunol. Immunopathol. **97**:125–136.
23. **Kilpatrick AM, et al.** 2006. Predicting the global spread of H5N1 avian influenza. Proc. Natl. Acad. Sci. U. S. A. **103**:19368–19373.
24. **King CA, Marshall JS, Alshurafa H, Anderson R.** 2000. Release of vasoactive cytokines by antibody-enhanced dengue virus infection of a human mast cell/basophil line. J. Virol. **74**:7146–7150.
25. **Korteweg C, Gu J.** 2008. Pathology, molecular biology, and pathogenesis of avian influenza A (H5N1) infection in humans. Am. J. Pathol. **172**:1155–1170.
26. **Lee DC, et al.** 2005. p38 mitogen-activated protein kinase-dependent hyperinduction of tumor necrosis factor alpha expression in response to avian influenza virus H5N1. J. Virol. **79**:10147–10154.
27. **Li X, McKinstry KK, Swain SL, Dalton DK.** 2007. IFN-gamma acts directly on activated CD4+ T cells during mycobacterial infection to promote apoptosis by inducing components of the intracellular apoptosis machinery and by inducing extracellular proapoptotic signals. J. Immunol. **179**:939–949.
28. **McKimm-Breschkin JL, Selleck PW, Usman TB, Johnson MA.** 2007. Reduced sensitivity of influenza A (H5N1) to oseltamivir. Emerg. Infect. Dis. **13**:1354–1357.
29. **Metcalfe DD, Baram D, Mekori YA.** 1997. Mast cells. Physiol. Rev. **77**:1033–1079.
30. **Metz M, Siebenhaar F, Maurer M.** 2008. Mast cell functions in the innate skin immune system. Immunobiology **213**:251–260.
31. **Minami M, et al.** 2002. Role of IFN-gamma and tumor necrosis factor-alpha in herpes simplex virus type 1 infection. J. Interferon Cytokine Res. **22**:671–676.
32. **Orinska Z, et al.** 2005. TLR3-induced activation of mast cells modulates CD8+ T-cell recruitment. Blood **106**:978–987.
33. **Palese P.** 2004. Influenza: old and new threats. Nat. Med. **10**:S82–S87.
34. **Puissant-Lubrano B, et al.** 2010. Control of vaccinia virus skin lesions by long-term-maintained IFN-gamma+TNF-alpha+ effector/memory CD4+ lymphocytes in humans. J. Clin. Invest. **120**:1636–1644.
35. **Salomon R, Hoffmann E, Webster RG.** 2007. Inhibition of the cytokine response does not protect against lethal H5N1 influenza infection. Proc. Natl. Acad. Sci. U. S. A. **104**:12479–12481.
36. **Shirato K, Taguchi F.** 2009. Mast cell degranulation is induced by A549 airway epithelial cell infected with respiratory syncytial virus. Virology **386**:88–93.
37. **Spender LC, Hussell T, Openshaw PJ.** 1998. Abundant IFN-gamma production by local T cells in respiratory syncytial virus-induced eosinophilic lung disease. J. Gen. Virol. **79**:1751–1758.
38. **St John AL, et al.** 2011. Immune surveillance by mast cells during dengue infection promotes natural killer (NK) and NKT-cell recruitment and viral clearance. Proc. Natl. Acad. Sci. U. S. A. **108**:9190–9195.
39. **Sun QH, Peng JP, Xia HF, Yang Y.** 2007. IFN-gamma promotes apoptosis of the uterus and placenta in pregnant rat and human cytotrophoblast cells. J. Interferon Cytokine Res. **27**:567–578.
40. **Sundstrom JB, Little DM, Villinger F, Ellis JE, Ansari AA.** 2004. Signaling through Toll-like receptors triggers HIV-1 replication in latently infected mast cells. J. Immunol. **172**:4391–4401.
41. **Szretter KJ, et al.** 2007. Role of host cytokine responses in the pathogenesis of avian H5N1 influenza viruses in mice. J. Virol. **81**:2736–2744.
42. **Uiprasertkul M, et al.** 2005. Influenza A H5N1 replication sites in humans. Emerg. Infect. Dis. **11**:1036–1041.

42a. **Wang D, et al.** 2008. Mast cell mediated inflammatory response in chickens after infection with very virulent infectious bursal disease virus. Vet. Immunol. Immunopathol. **124**:19–28.

43. **Wong SS, Yuen KY.** 2006. Avian influenza virus infections in humans. Chest **129**:156–168.
44. **Xu T, et al.** 2006. Acute respiratory distress syndrome induced by avian influenza A (H5N1) virus in mice. Am. J. Respir. Crit. Care Med. **174**:1011–1017.
45. **Zhao Y, et al.** 2008. Neutrophils may be a vehicle for viral replication and dissemination in human H5N1 avian influenza. Clin. Infect. Dis. **47**:1575–1578.
46. **Zhou Y, Weyman CM, Liu H, Almasan A, Zhou A.** 2008. IFN-gamma induces apoptosis in HL-60 cells through decreased Bcl-2 and increased Bak expression. J. Interferon Cytokine Res. **28**:65–72.